Effect of Respirophasic Displacement of the Inferior Vena Cava on Size Measurement in 2-D Ultrasound Imaging

Ultrasound in Medicine & Biology 50 (2024) 1785–1792

Contents lists available at ScienceDirect

Ultrasound in Medicine & Biology

journal homepage: www.elsevier.com/locate/ultrasmedbio

Original Contribution

Effect of Respirophasic Displacement of the Inferior Vena Cava on Size Measurement in 2-D Ultrasound Imaging

Piero Policastro [a], Leonardo Ermini [b], Stefania Civera [c], Stefano Albani [c,1], Giuseppe Musumeci [c], Silvestro Roatta [b], Luca Mesin [a,*]

[a] Mathematical Biology and Physiology, Department of Electronics and Telecommunications, Politecnico di Torino, Turin, Italy
[b] Department of Neuroscience, University of Torino, Turin, Italy
[c] Division of Cardiology, Ospedale Ordine Mauriziano di Torino, Turin, Italy

ARTICLE INFO

Keywords:
Inferior vena cava
Ultrasound
Tracking

ABSTRACT

Objective: Volume status assessment of a patient by ultrasound (US) imaging of the inferior vena cava (IVC) is important for the diagnosis and prognosis of various clinical conditions. In order to improve the clinical investigation of IVC, which is mainly based on unidirectional US (in M-mode), automated processing of 2-D US scans (in B-mode) has enabled tissue movement tracking on the visualized plane and can average this in various directions. However, IVC geometry outside of the visualized plane is not under control and could result in errors that have not yet been evaluated.

Methods: We used a method that integrates information from long- and short-axis IVC views (simultaneously acquired in the X-plane) to assess challenges in IVC diameter estimations using 2-D US scans in eight healthy subjects.

Results: Relative movements between the US probe and IVC induced the following problems when assessing IVC diameter *via* 2-D view: a median error (*i.e.*, absolute difference with respect to diameter measured in the X-plane) of 17% using 2-D US scans in the long-axis view of the IVC affected by medio-lateral displacements (median: 4 mm); and a median error of 7% and 9% when measuring the IVC diameter from a short-axis view in the presence of pitch angle (median: 0.12 radians) and cranio-caudal movement (median: 15 mm), respectively.

Conclusion: Relative movements in the IVC that are out of view of B-mode scans cannot be detected, which results in challenges in IVC diameter estimation.

Introduction

Ultrasound (US) scanning is an important medical imaging method due to its non-invasiveness and cost-effectiveness [1,2]. In recent years, this imaging technique has gained remarkable importance in medical structures due to increased machine performance, *e.g.*, in terms of spatial [3] and temporal resolution [4]. X-plane (or biplane) recordings allow physicians to simultaneously acquire images of the same tissue in two perpendicular planes, enabling accurate analysis of complex structures [5].

Veins are blood vessels that return blood to the heart. They have a low internal pressure and are characterized by a prominent ability to dilate (*i.e.*, they have great compliance), and may thus accommodate and eventually redistribute large volumes of fluid [6]. Both arteries and veins have three layers, but arteries have a thicker middle layer in order to cope with higher blood pressure. Veins are thinner and less stiff, so they are more likely to change shape due to variations in transmural pressure.

The inferior vena cava (IVC), the biggest vein vessel in the human body, is linked directly to the right atrium. Diameter variations within the IVC reveal important information about the volume as well as central venous pressure status of the subject [7,8]. Specifically, the caval index (CI) is commonly used to assess IVC collapsibility, which correlates with volume status [9] and right atrial pressure [10]. The CI is obtained by measuring the maximum and minimum diameters of the IVC [11]. However, assessment of IVC size (and hence also evaluation of CI) is not standardized [12]; thus, the measured values could be subject to error [13]. As a consequence, poor accuracy is achieved when IVC indices are used to estimate volume responsiveness [14] and right atrial pressure [15]. Some causes of error are related to the following factors:

* Corresponding author. Dipartimento di Elettronica e Telecomunicazioni, Politecnico di Torino, Corso Duca degli Abruzzi, 24 - 10129 Torino, Italy.
E-mail address: luca.mesin@polito.it (L. Mesin).
[1] Current affiliation: Division of Cardiology, Umberto Parini Regional Hospital, Aosta, Italy.

https://doi.org/10.1016/j.ultrasmedbio.2024.07.005
Received 7 November 2023; Revised 10 July 2024; Accepted 15 July 2024

1. The use of M-mode visualization, which selects a fixed US line, making the method prone to respirophasic IVC movements [16,17]
2. Differing modalities of respiration between patients [18]
3. Operator experience [13]
4. The complicated geometry of the IVC and varying collapsibility in different directions along its longitudinal axis [19] and cross-section [20]
5. 3-D movement of the IVC relative to US probe orientation, including both cranio-caudal and medio-lateral displacements [11], together with rotations in different planes [21]

Several algorithms have been developed for IVC segmentation to address some of these challenges. These algorithms analyze a single IVC view in B-mode, either longitudinal or transversal to the blood vessel [17,22,23]. Visualization in the X-plane allows the identification of IVC movements in the longitudinal and transverse directions at the same time [21]. An algorithm that integrates information from longitudinal and transverse views of the IVC to compensate for motion that adversely affects measurements from a single B-mode scan has been described by Policastro and Mesin [21]. In the simulated videos, this algorithm showed impressive performance in mean diameter estimation (with a maximum error of 2% relative to the simulated ground truth), correctly compensating for artifacts caused by relative movements between the IVC and probe.

Here, we document errors in IVC size estimation when using US scans from a single view in the presence of specific IVC movements, using the algorithm compensating for them as a reference [21]. Specifically, we focus on the following important IVC displacements: medio-lateral translations, rotation in the longitudinal plane (measured by pitch angle) and longitudinal translations. Notice that the reference algorithm, integrating long- and short-axis views of the IVC, was tested on simulated videos in which there was a single vein movement at a time [21]. In real US acquisitions, all three movements can be overlaid and displayed concurrently with changes in vein size. Therefore, predicting the effect of each individual factor in an experimental setting is not easy.

Thus, the aim of this paper was to analyze real data and assess the effects of specific IVC movements on the estimation of size using US scans from individual B-planes. In fact, there are IVC movements that cannot be appreciated on the single 2-D view. However, simultaneously monitoring IVC position and movements on a second 2-D plane perpendicular to the first plane allows the detection and correction (in part) of possible errors in diameter assessment from single 2-D views. Thus, errors in IVC size monitoring from single 2-D views (related to IVC movements, which are visible only out of the plane of view) are quantified using the new algorithm as a reference [21], which integrates information from long- and short-axis views acquired by X-plane scans.

Materials and methods

We enrolled eight healthy subjects. The Mauriziano Hospital (Turin) Ethics Committee approved the study (approval number 388/2020; experimental protocol identifier v.1, 1 June 2020) and informed consent was obtained according to the policies of the institutional review board. Anonymization was applied to protect patient data. For each patient, an X-plane US video, which provides two simultaneous views of the same target in perpendicular US planes, was acquired using a GE Vivid E95 (GE Healthcare, Vingmed Ultrasound, Horten, Norway). The output of the segmentation algorithms in the long [19] and short axes [20] was provided as input for our 3-D estimation algorithm (implemented in Matlab, Mathworks, Natick, MA, USA) in order to extract IVC size measurements from a combination of the two views [21].

Analysis of data and management of outliers

Diameters were estimated for each frame of the acquired US video clips, using either of the following three methods:

1. Long-axis view: an average of estimations along the IVC course in a direction orthogonal to the axis, as in [19].
2. Short-axis view: the equivalent diameter was estimated from the cross-sectional area of the IVC, as in [20].
3. X-plane: the method proposed in [21] was used, which integrates information from both long- and short-axis views.

Differences between estimations were then obtained subtracting those from the 2-D views (either in long or short axis) and those given by the method in [21]. These estimation differences were investigated as a function of different movements of the IVC with respect to the probe: transverse translation, pitch angle and longitudinal displacement.

Some diameter estimations, when displayed in relation to specific IVC movements, showed a large deviation from the main trend. This could be due to either noisy frames making mistakes during processing or peculiar relative locations of the probe with respect to the IVC; *e.g.*, significant influences of other geometrical parameters or an out-of-plane rotation. In fact, various tissue movements (translations, rotations, etc.) and deformations (collapsibility) occurred together in experimental data. These particular diameter estimations were considered outliers and removed, as they have the potential to affect interpretation of the effects of the specific geometrical parameter of interest. We identified the outliers using the isolation forest algorithm [24]: binary trees were used to isolate the data and those requiring fewer splits were given higher anomaly scores; outliers were identified as the 10% of data with the largest anomaly scores.

Tests

The effect of three possible IVC movements, measured individually and correlated with diameter estimation error, were investigated as follows:

1. Medio-lateral translations. IVC movements were easily visible in the transverse section but they were not noticeable in the long-axis view, where they induced an underestimation bias in the size, which is more important as the section was further from the center of the vein.
2. Variation in the pitch angle value. This could be compensated for in the longitudinal section by IVC tracking. On the other hand, it was not visible in the short-axis view and it had the effect of overestimating the transverse diameter (with a larger effect when the section was further from occurring orthogonal to the IVC axis).
3. Longitudinal translations. These were noticeable in the longitudinal section, where they could be compensated by IVC tracking. An error in diameter estimation was found in the transverse view if the size of the vein changed along its longitudinal course.

The percentage errors when using the 2-D measurement (*i.e.*, in the long- or short-axis views) were computed using the diameter estimated by integrating information from the long- and short-axis views as the reference (referred to as 'equivalent 3-D diameter'), as shown in Equations 1 and 2:

$$\text{error}_{\text{long}} = 100 \times \frac{\text{equivalent diameter}_{\text{long}} - \text{equivalent 3D diameter}}{\text{equivalent 3D diameter}} \quad (1)$$

$$\text{error}_{\text{transv}} = 100 \times \frac{\text{equivalent diameter}_{\text{transv}} - \text{equivalent 3D diameter}}{\text{equivalent 3D diameter}} \quad (2)$$

where equivalent $\text{diameter}_{\text{long}}$ and equivalent $\text{diameter}_{\text{transv}}$ are the measurements obtained by averaging the diameters estimated in the long-axis view (in different locations along the IVC course, in a direction orthogonal to the axis, as in [19]) and in the short-axis view (obtained from the cross-sectional area, as in [20]), respectively.

Analysis of the results

The percentage errors of the 2-D versus 3-D equivalent diameters (estimated for each frame of US scans) were displayed in scatter plots showing their relation to the three investigated IVC movements. Data (after excluding outliers) were interpolated with a line indicating the standard error.

Moreover, the observed movement and maximal percentage error ranges were investigated.

From the equivalent diameter obtained by either of the three methods, the CI, respiratory CI (RCI) and cardiac CI (CCI) were computed (as in the previous work [13]). For each time series of equivalent diameter, more indexes were estimated (*i.e.*, CI and RCI were estimated for each respiratory cycle, and CCI was computed for each heartbeat). They were then averaged, obtaining single values (for an all-time series of equivalent diameter) which were compared.

Finally, mean diameters and collapsibility indexes were explored, and their possible differences among estimation methods (*i.e.,* 2-D long- and short-axis views or X-plane) investigated using the Wilcoxon signed rank test for paired comparisons.

Results

We studied the contributions of three geometrical factors toward IVC diameter estimation errors using longitudinal and transverse views. Each of these factors is examined in detail here, showing specific examples first (in Figs. 1–3) and then the overall results (in Figs. 4–8).

Figure 1 shows a subject characterized by prominent medio-lateral movements of the IVC and for whom the diameters estimated by different methods differ significantly. Two frames were selected, in which the displacement of the longitudinal plane from the IVC center was either the smallest or the largest. The three estimated diameters are displaced over time at the bottom of the figure. The corresponding time of the two frames reported above has been highlighted. The differences in diameters estimated from the long-axis, short-axis and X-plane views were minimal when the center of the IVC was close to the tilt line indicating the long-axis section but were significant at maximum translation. The equivalent 3-D diameter was estimated by compensating for medio-lateral translation using the short-axis view. We can therefore assume that it was not affected by medio-lateral translation, contrary to the longitudinal diameter, which behaved very differently from cross-section estimations when displacement was large.

The effect of the estimated IVC rotation in the long-axis plane (*i.e.*, the pitch) on diameter measurement is shown in Figure 2. Again, two frames were selected to show different conditions: the first frame, where the longitudinal axis of the IVC shows some pitch angle with the tilt line indicating the direction of the short-axis section; and the second frame, in which they are almost perpendicular. Due to the pitch angle visible in the longitudinal view, the cross-section is larger than when it is taken orthogonal to the IVC axis so that the equivalent diameter estimated from the short-axis view has a positive bias, as shown in the traces reported in the lower part of Figure 2. The equivalent diameter obtained from processing the two sections from the X-plane view compensates for the effect of this error. Notice that when the transverse section is orthogonal to the IVC axis (*i.e.*, for the second frame), the three estimated diameters are almost identical.

The third case, *i.e.*, longitudinal translation, is shown in Figure 3. An IVC with a conical shape, as for the subject chosen for this figure, emphasizes the effect of this cranio-caudal translation. Two frames were chosen where the relative translation of the cross-section was quite large. The three diameter estimations (by 2-D view in B-mode in the long and short axes and X-plane) were almost identical in the first frame, but the translation largely affected the cross-section in the second frame.

An interesting common thread was noted in the specific examples shown in Figures 1–3 (which is seen again later in Fig. 8 when the entire dataset is considered): the long-axis view generally produced smaller estimates than the short axis, as the first view could be negatively biased by medio-lateral displacement, whereas the second view was positively biased by a pitch rotation with respect to the IVC axis (both problems were not visible from the corresponding view).

Figures 4–6 show the overall results of the entire dataset, considering the same IVC movements as in the specific examples shown in Figures 1–3, respectively. The dynamics of the IVC are quite complex, as different translations and rotations occur simultaneously and together with variations in size. Moreover, IVC movements and size variation are usually correlated, as they are both related to the respiratory cycle. Thus, to attempt to determine the possible effect of specific movements on diameters estimated from long- and short-axis views, these estimations were referred to the value computed by the new algorithm (applied to X-plane US scans), which compensates for their effects. Therefore, the

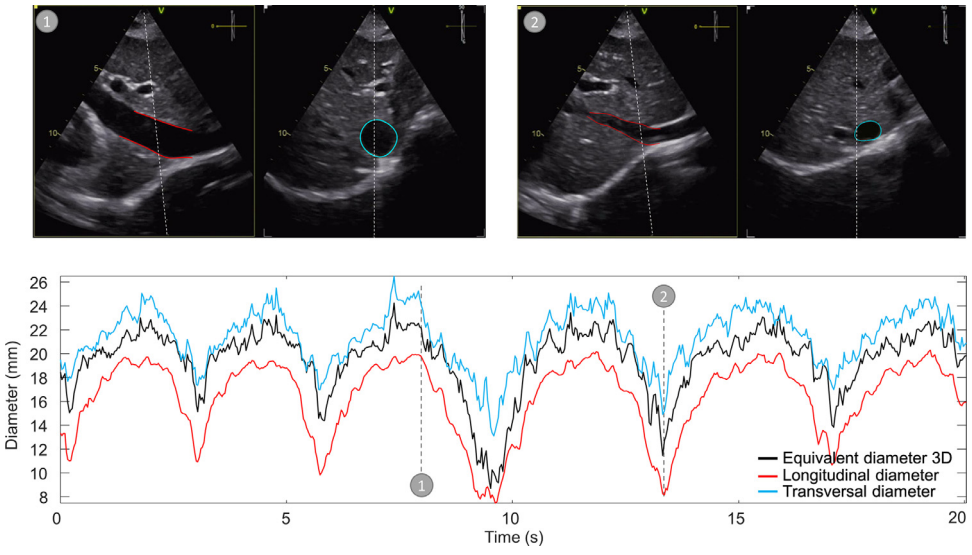

Figure 1. Estimation of the diameter of the inferior vena cava (IVC) in subject 5, in which the vein makes a large medio-lateral movement. The top panels display two X-plane echography images of the IVC, in which the long-axis section is taken either close to the center of the cross-section (*left*) or close to the border (*right*). The time course of the diameter is shown in the bottom panel, estimated from the longitudinal and transverse views and by integrating their information. The times at which the frames shown on top occurred are indicated in the bottom graph. A small diameter is estimated from the long-axis view when the medio-lateral translation is large.

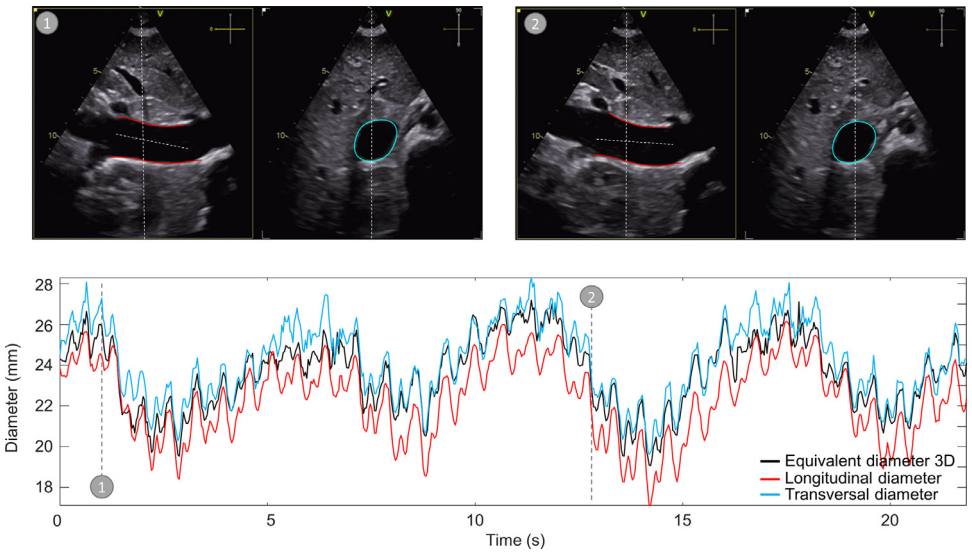

Figure 2. Estimation of inferior vena cava (IVC) diameter in subject 4, in which the vein makes an in-plane rotation. The top panels display two X-plane echography images of the IVC, in which the angle between the short-axis section and the vein is small (*left*) or close to 90 (*right*). The time course of the diameter is shown in the bottom panel, estimated from the longitudinal and transverse views and by integrating their information. The times at which the frames shown on top occurred are indicated in the bottom graph. The diameter estimated from the short-axis view has a positive bias when the angle is smaller.

percentage error, given in either Equation 1 or 2, was plotted versus the different movements.

Specifically, Figure 4 shows a scatter plot for each of the eight subjects. The percentage error of the diameter estimate of the long axis was given for each frame of the video as a function of the relative medio-lateral displacement of the IVC from its center with respect to the transverse diameter. Notice that relative displacement was shown, as a dimensional translation (*i.e.*, given in mm) has a different effect depending on the size of the cross-section. Considering also that the diameter of the IVC can vary substantially between subjects and as a result of IVC collapsibility, only displacements relative to IVC size were able to fairly demonstrate their effect.

In Figure 5 the percentage error in diameter estimation in the short-axis view is shown in scatter plots (one for each subject) versus the pitch angle in radians (with zero corresponding to a tilt line orthogonal to the IVC axis). A positive bias in the short-axis estimation of IVC size was expected when the pitch angle was further from zero. Note that there was occasionally an offset, which indicated an error even when the pitch angle was close to zero. As the short-axis view does not have access to longitudinal cross-sectional information, there could be changes outside the cross-sectional plane that would account for the observed bias. For example, the null pitch condition could apply when the IVC shifted to a region where it was on average larger or smaller than its average size in the region analyzed by the 3-D approach.

Scatter plots for each subject are shown in Figure 6, with the longitudinal translation (mm) shown along the x-axis (considering the translations toward the region in which the dimension of the IVC was larger in the average shown across the frames of the echography as positive) and

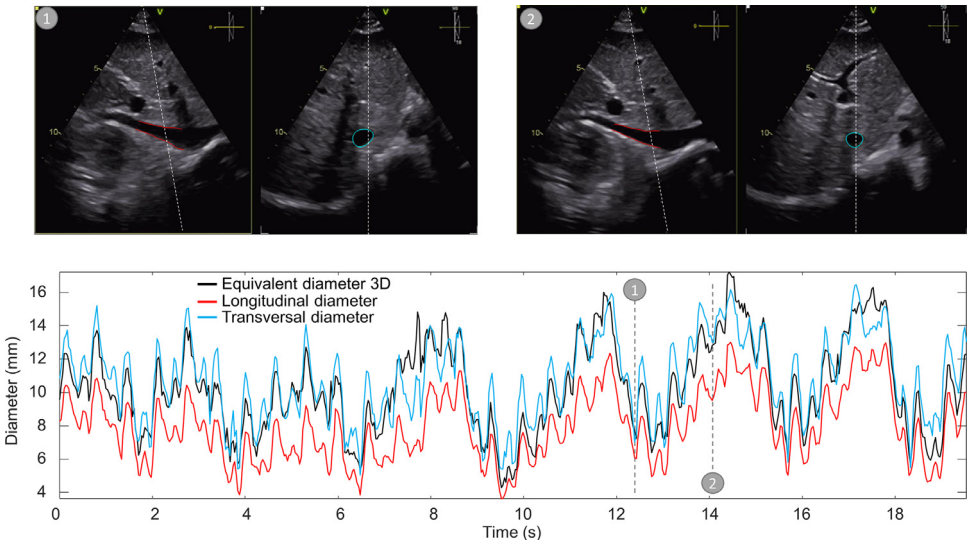

Figure 3. Estimation of inferior vena cava (IVC) diameter in subject 1, in which the vein has large variations of the section in its long-axis course. The top panels display two X-plane echography images of the IVC, in which the translation of the vein causes the short-axis section to be taken either where it is smaller (*left,* cranial direction) or larger (*right*, caudal). The time course of the diameter is shown in the bottom panel, estimated from longitudinal and transverse views, and by integrating their information. The times at which the frames shown on top occurred are indicated in the bottom graph. In this case, the diameter estimated from a short-axis view has a positive bias when the IVC moves in the caudal direction.

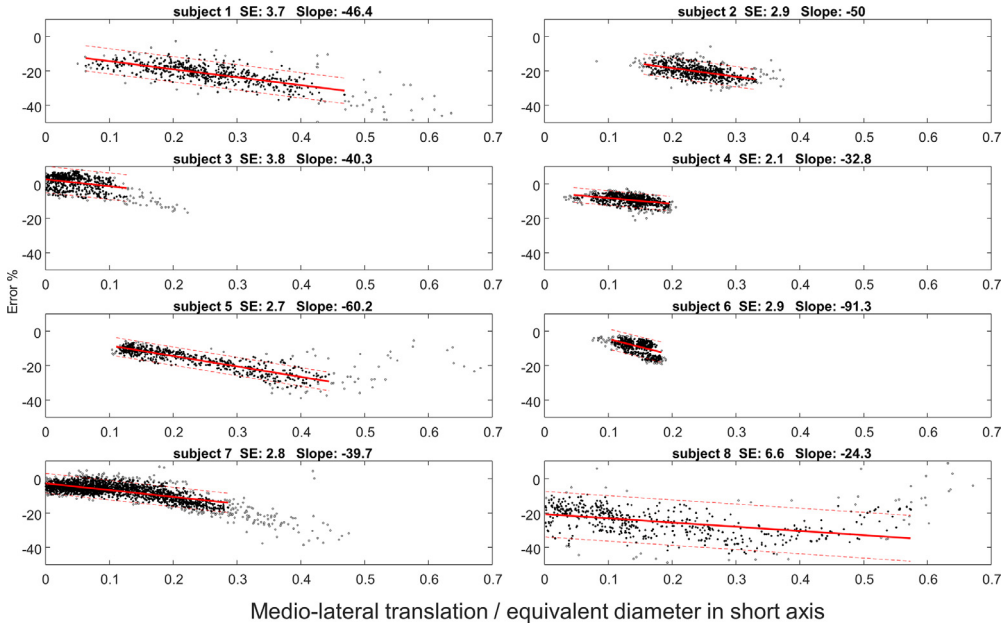

Figure 4. Percentage error of the diameter derived from the longitudinal section relative to the equivalent diameter recovered from inferior vena cava volume estimation, shown as a function of medio-lateral translation. All frames and subjects are considered. The x-axis shows the ratio of the medio-lateral translation with respect to the tilt line to the diameter calculated from the transverse section. The linear interpolation is shown by a red line and the range defined by the standard error is indicated by a red dotted line, after removing the outliers. The identifier of the subjects, the standard error and the slope of the interpolation line are indicated in the title.

the percentage error in the estimation of the diameter from the short-axis view along the y-axis.

Figure 7 shows the three different movement ranges and the maximum errors observed in the subjects. Respiratory cycles are the principal cause of IVC movement, with the greatest excursion range occurring between inspiration and expiration. We expected that the maximum errors could occur at the maximum movement excursions: this is the rationale that relates maximum errors to range of movement. Parameters were computed as 90% percentiles (after removing outliers) in order to obtain robust estimations.

Pitch angle has never been documented before. It is a small rotation but it can have a discreet effect when taking measurements in the short-axis view. Median maximal errors were approximately 17% for the long-axis measurement affected by a medio-lateral movement; when using the short-axis view, errors were approximately 7% and 9% for pitch angle and cranio-caudal translation, respectively. Median cranio-caudal

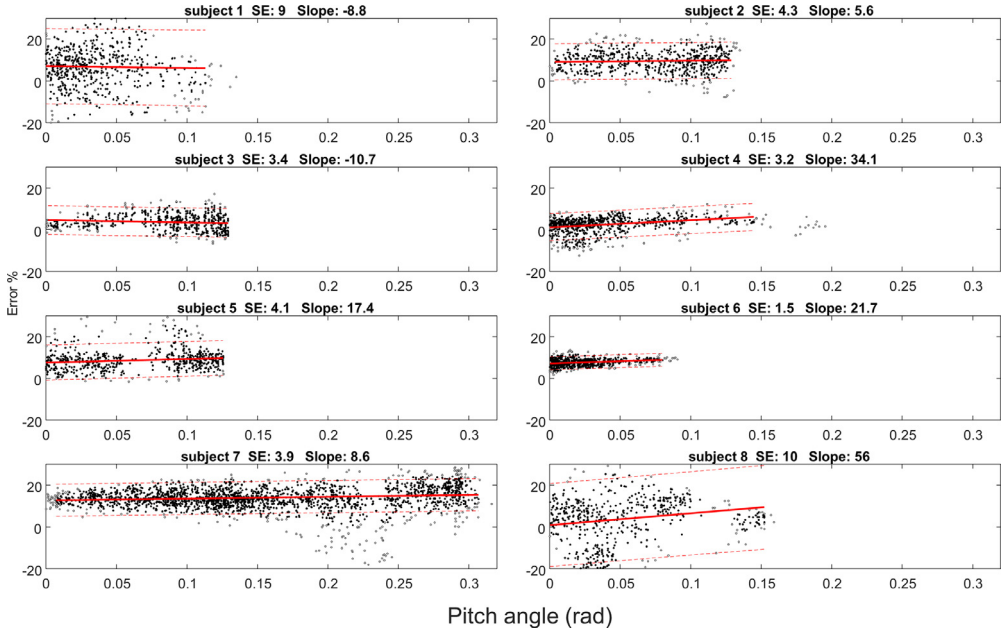

Figure 5. Percentage error of the diameter derived from the transverse section relative to the equivalent diameter recovered from inferior vena cava volume estimation, shown as a function of the absolute value of the pitch angle. All frames and subjects are considered. The x-axis shows the pitch, in radians, with respect to the perpendicular tilt line. Linear interpolation is shown by a red line and the range defined by the standard error is indicated by a red dotted line, after removing the outliers. The identifier of the subjects, the standard error, and the slope of the interpolation line are indicated in the title.

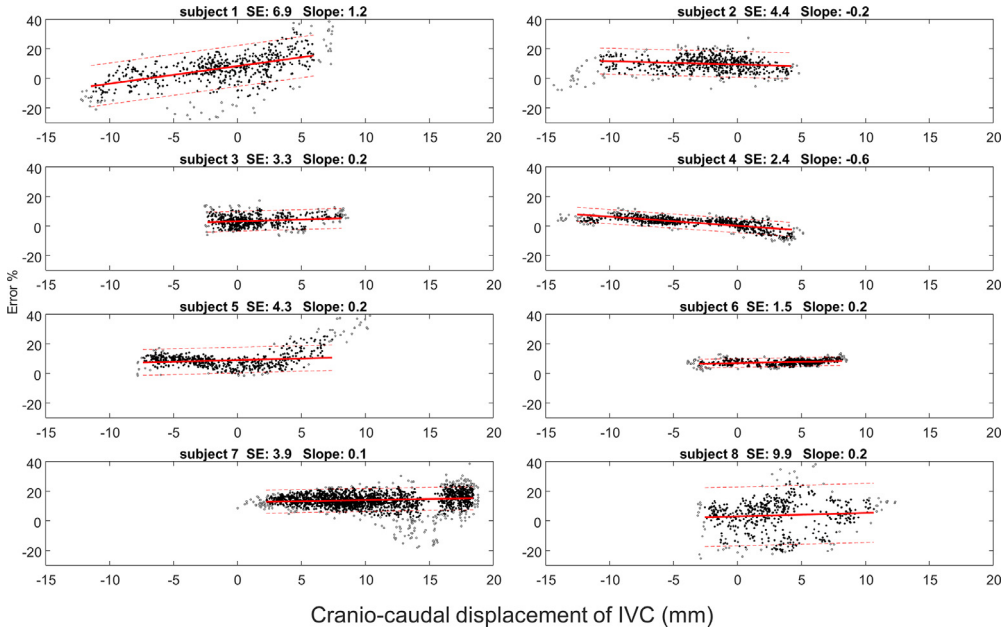

Figure 6. Percentage error of the diameter derived from the transverse section relative to the equivalent diameter recovered from inferior vena cava volume estimation, shown as a function of longitudinal translations. All frames and subjects are considered. The x-axis shows the longitudinal translations with respect to the tilt line (mm). Linear interpolation is shown by a red line and the range defined by the standard error is indicated by a red dotted line, after removing the outliers. The identifier of the subjects, the standard error, and the slope of the interpolation line are indicated in the title.

and medio-lateral translations were 15 and 4 mm, respectively, and the median pitch angle was 0.12 rad.

The implications of using a 2-D scan (in long- or short-axis views) instead of a 3-D scan (X-plane view) on the estimation of parameters of clinical interest are shown in Figure 8. As already outlined in Figures 1–7, the IVC diameter tended to be underestimated in the long-axis view, whereas it was overestimated when using the short-axis view (both variations with respect to the X-plane estimation were statistically significant, according to the Wilcoxon signed rank test; notice that the diameter estimated in the short axis was always the largest, showing high significance in paired comparisons). Collapsibility indexes appeared to show less consistent variations, even if on average there was a small (not significant) positive bias in measuring the CI and RCI in the long-axis view versus the 3-D approach. CI and RCI estimations *via* long-axis views also showed quite a large variation with respect to using the 3-D information provided by the X-plane view. In fact, the range of differences was approximately 20% (notice that the median CI was approximately 25% and 33% for the X-plane and long-axis views, respectively, with the result that the uncertainty was a rather large proportion of the value measured). Instead, the range of differences in CI and RCI

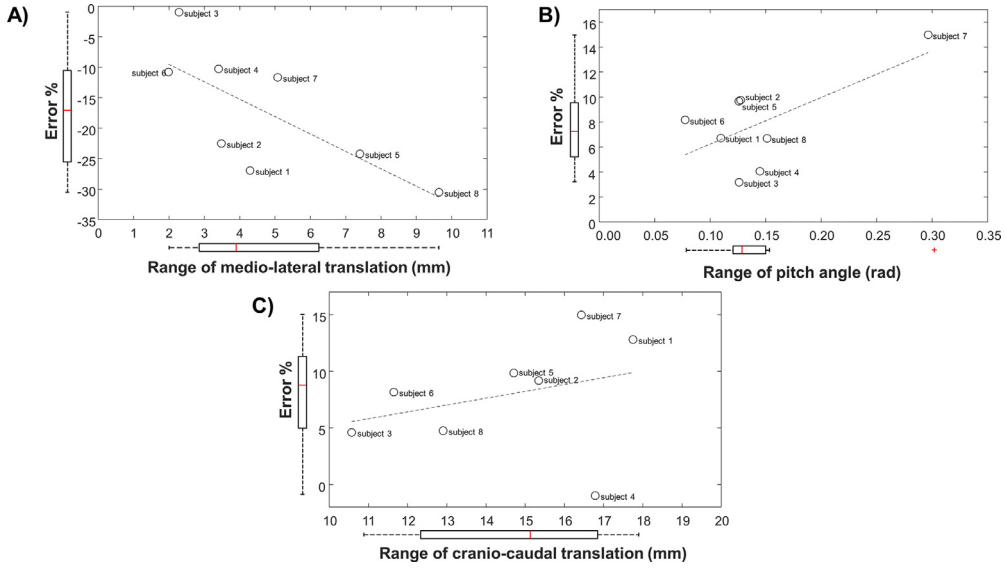

Figure 7. Range of movements and percentage errors (ErrL and ErrT indicating the error when using the long- and short-axis view, respectively) observed in different subjects (scatter plots of a pair of variables and boxplot of each variable). (a) Error in the estimation of the diameter from the long-axis view over the medio-lateral translation. For each subject, the maximal error (outlier excluded) and the maximal translation in millimeters are considered. A scatter plot and boxplot of each variable are shown. (b) Error in the estimation of the diameter from the short-axis view over the pitch angle (same format as in [a]). (c) Error in the estimation of the diameter from the short-axis view over the cranio-caudal translation.

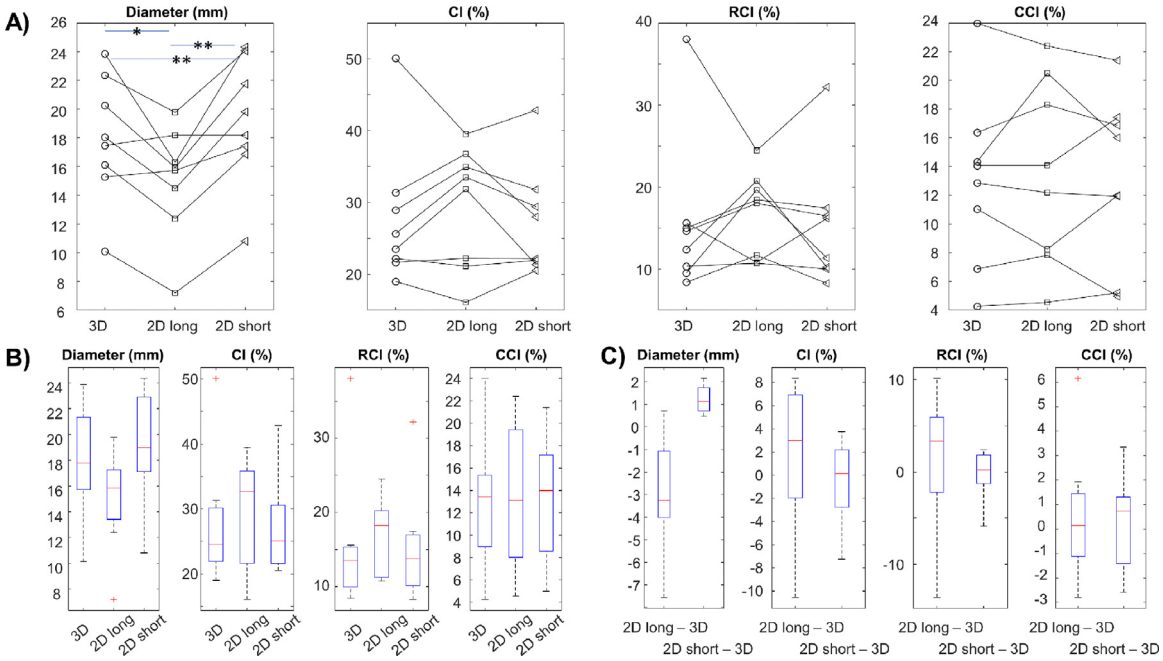

Figure 8. Estimation of inferior vena cava parameters (*i.e.*, mean diameter, caval index [CI], respiratory caval index [RCI] and cardiac caval index [CCI]) using ultrasound scans in the X-plane (3-D), long-axis view (2-D long) and short-axis view (2-D short). (a) Individual parameters (mean diameter, CI, RCI and CCI) estimated from each subject using the three methods (3-D, 2-D long and 2-D short). Statistical differences were found for diameter measurements ($*p < 0.05$ and $**p < 0.005$). (b) Box and whisker plots (showing the median, quartiles, range and outliers) of estimations of the parameters with the three methods. (c) Box and whisker plots showing differences in estimations of the parameters when using the 2-D method instead of the 3-D method.

estimations was approximately 10% for the short-axis view. The CCI showed lower estimation differences, but the range of values measured was also smaller.

Discussion

The IVC shows large movements during respiration as it is attached to the diaphragm as well as other tissues. Moreover, the skin surface over which the probe is placed is also affected by large respirophasic movements. Therefore, achieving a US scan of a particular area during the respiratory cycle can be challenging. In fact, while B-mode visualization and image-processing techniques are able to compensate for in-plane movements, the 3-D geometry and movements of the IVC can also develop partly outside the scanned view.

In this paper, we used visualization in the X-plane to detect and compensate for IVC spatial orientation and movements. Using the X-plane as a reference, we documented the measurement errors expected in simple 2-D visualization (in either the short or long axis).

Figure 1 clearly shows the effect of medio-lateral translation on the diameter estimated from the longitudinal view. The effect of this movement could be mitigated when integrating information from the short-axis view. Movement is mainly caused by breathing causing movement of the abdomen (on which the probe is placed); therefore, it is not easy to maintain an IVC axis on the 2-D longitudinal plane by manually adjusting probe orientation. In fact, the IVC collapses at the same time it moves, thus it is not easy to determine whether size changes are attributable only to collapsibility or to medio-lateral displacement from the long-axis view.

In the lower part of Figure 1, the diameters estimated from the three different sources are almost the same at point 1 (when the tilt plane in the transverse plane is close to the center of the cross-section), but there are some differences at point 2. In fact, in the second selected point, the transverse section line is close to the vein wall. If movement is greater than the cross-sectional radius, it can cause the vein to disappear in the longitudinal view (leading the operator to suspect complete collapse).

An important pitch rotation of the IVC in the plane of the long axis was seen in only a few subjects involved in this study. However, its effect clearly distorted the visualized cross-section. For example, in the ideal case in which the IVC is a cylinder with a circular section, the visualized cross-section is an ellipse with larger eccentricity as the angle increases. Figure 2 shows this problem, considering two frames in which the short-axis section is either close or far from being orthogonal to the IVC axis.

Cranio-caudal movement of the IVC is most evident during respiration as the vein is attached to the diaphragm. However, it has an important effect on estimations of IVC size along the cross-section only if the vein presents substantial size changes along its length (or if it is associated with a pitch rotation). Figure 3 shows an example of the IVC with size changes along its course: as the short-axis section is fixed, cranio-caudal movement causes the US plane to intersect the vein at different sites, thus producing only apparent size changes. Integration of the information from the two sections allows the new algorithm based on the X-plane view to compensate for this problem.

From a quantitative point of view (Figs. 4–6), the medio-lateral (Fig. 4) and cranio-caudal movements detected (Fig. 6) are compatible with the study by Blehar et al. [11]. Pitch angle, however, has thus far never been documented in the literature.

Interpretation of the results must be done with caution, as the various movements and size variations occur together and may be linked. In addition, it is possible that some frames were taken out of the plane (*i.e.*, at a yaw angle), causing the reference algorithm (based on the X-plane view) to also fail. In a few cases the results differed from those expected. However, the average behavior across subjects is in line with our expectations and easily interpreted in simulated conditions [21], *i.e.*, the diameter is underestimated in the long axis in case of medio-lateral translation and overestimated in the short axis for large pitch angles and cranio-caudal translations toward the region in which the IVC is larger. This is found in the overall results shown in Figure 7, which summarizes the magnitude of each movement investigated, showing the distribution of the values observed in the subjects included in the study. The three movements are considered in different panels, showing scatter plots of the maximal percentage error versus the range of movements and the

boxplots of each variable. The median errors (approximately 17% for the long-axis measurement with medio-lateral movement; and 7% and 9% in the short axis for pitch angle and cranio-caudal translation, respectively) indicate some limitations in the accuracy with which the size of the IVC can be estimated using a single US section. This could have implications for the measurement repeatability [13]. We expect that the observed errors could depend on the operator and the subject (as indicated by the large ranges in variation), as various factors are involved such as IVC anatomy and the relative motion between the IVC (affected by the modality of respiration, tissue compliance, etc.) and the probe (handled by an operator trying to accommodate abdomen movements during respiration). However, on average these errors have consistent dependencies on movement, which is in line with the results of the theoretical part of our work [21]. During simulations each movement could be considered separately, one at a time, documenting the individual effects; however, in experimental data, other concomitant motions or deformations could obscure interpretation of the results. However, our experimental results were still able to correlate with the simulations. In fact, it is clear that IVC size estimation is affected by movements not identifiable in a single plane of view. Therefore, caution in the interpretation of measurements is recommended when measuring the IVC using a 2-D view. It is hoped that the increased use of US systems for X-plane visualization and 3-D estimation will help to reduce errors and limit measurement variability, which is still the most important limitation of this noninvasive assessment of IVC.

Challenges in measuring IVC size using 2-D US visualizations are reflected in the estimation of collapsibility indexes (*i.e.*, CI, RCI and CCI). The largest variation was found in CI and RCI estimations, which are directly affected by the respiratory cycle. Our data showed some variability in the estimations, but no statistically significant differences with respect to assessment in the X-plane, nor a clear trend nor bias. In fact, movements and size variations were correlated; thus, depending on the relative position of the probe and the IVC, the contributions to size changes from movement and respiration-induced pressure variations could accumulate or be in counterphase. This introduces variations in the estimation of CIs from the different views that are not consistent across different subjects, which could in part justify the poor repeatability of collapsibility assessments of IVCs documented in the literature [13].

Given the problems in estimating IVC dynamics from 2-D views (either in the long or short axis), the 3-D approach could be a potentially useful alternative if systems that provide visualization in the X-plane become widespread. Assessing its benefits remains for future investigations. For example, it would be interesting to test possible improvements in definitions of the clinical picture (*e.g.*, in diagnosing volume status or measuring right atrial pressure) or repeatability of the estimates obtained using the new algorithm processing the X-plane view.

Conclusion

The evaluation of IVC size from longitudinal and transverse views is affected by vein movements that cannot be observed in the plane of the US scan. This challenge could be mitigated by integrating information from the two planes, which is synchronously acquired by a US system in the X-plane. Specifically, the algorithm introduced in [21] was able to compensate for medio-lateral translation, mean longitudinal axis pitch and longitudinal translation, and was used as a reference to document the effect of those movements in limiting the accuracy when evaluating IVC size and collapsibility in experimental data from single tilt sections. Specifically, for the first time this study simultaneously quantified three movements of the IVC on experimental US scans and confirmed the effects of the errors that characterize 2-D assessments.

Conflict of interest

An instrument implementing the 2-D algorithms used in this paper was patented by Politecnico di Torino and Università di Torino (patent number WO 2018/134726) and was taken in license by VIPER s.r.l.

Data availability statement

Data are available from the corresponding author upon reasonable request.

References

[1] Lentz B, Fong T, Rhyne R, Risko N. A systematic review of the cost-effectiveness of ultrasound in emergency care settings. Ultrasound J 2021;13(1):16.
[2] Zhang Y, Begum HA, Grewal H, Etxeandia-Ikobaltzeta I, Morgano GP, Khatib R, et al. Cost–effectiveness of diagnostic strategies for venous thromboembolism: a systematic review. Blood Adv 2022;6(2):544–67.
[3] Hasegawa H. Improvement of range spatial resolution of medical ultrasound imaging by element-domain signal processing. Japan J App Physics, 56; 2017. p. 201707JF02.
[4] Ng A, Swanevelder J. Resolution in ultrasound imaging. Contin Educ Anaesth Crit Care Pain 2011;11(5):186–92.
[5] Convissar D, Bittner EA, Chang MG. Biplane imaging versus standard transverse single-plane imaging for ultrasound-guided peripheral intravenous access: a prospective controlled crossover trial. Crit Care Explor 2021;3(10):e545.
[6] Mesin L, Albani S, Policastro P, Pasquero P, Porta M, Melchiorri C, et al. Assessment of phasic changes of vascular size by automated edge tracking-state of the art and clinical perspectives. Front Cardiovasc Med 2022;8:775635.
[7] Albani S, Mesin L, Roatta S, De Luca A, Giannoni A, Stolfo D, et al. Inferior vena cava edge tracking echocardiography: a promising tool with applications in multiple clinical settings. Diagnostics 2022;12:427.
[8] Policastro P, Mesin L. Processing ultrasound scans of the inferior vena cava: techniques and applications. Bioengineering 2023;10:1076.
[9] Mesin L, Roatta S, Pasquero P, Porta M. automated volume status assessment using inferior vena cava pulsatility. Electronics 2020;9(10).
[10] Mesin L, Albani S, Sinagra G. Non-invasive estimation of right atrial pressure using inferior vena cava echography. Ultrasound Med Biol 2019;45(5):1331–7.
[11] Blehar DJ, Resop D, Chin B, Dayno M, Gaspari RB. Inferior vena cava displacement during respirophasic ultrasound imaging. Crit Ultrasound J 2012;4(18):1–5.
[12] Wallace D, Allison M, Stone MB. Inferior vena cava percentage collapse during respiration is affected by the sampling location: an ultrasound study in healthy volunteers. Acad Emerg Med 2010;17(1):96–9.
[13] Mesin L, Giovinazzo T, D'Alessandro S, Roatta S, Raviolo A, Chiac-chiarini F, et al. Improved repeatability of the estimation of pulsatility of inferior vena cava. Ultrasound Med Biol 2019;45:2830–43.
[14] Orso D, Paoli I, Piani T, Cilenti FL, Cristiani L, Guglielmo N. Accuracy of ultrasonographic measurements of inferior vena cava to determine fluid responsiveness: a systematic review and meta-analysis. J Intens Care Med 2020;35:354–63.
[15] Magnino C, Omedè P, Avenatti E, Presutti DG, Iannaccone A, Chiarlo M, et al. Inaccuracy of right atrial pressure estimates through inferior vena cava indices. The Am J Cardiol 2017;120(9):166773.
[16] Mesin L, Pasquero P, Albani S, Porta M, Roatta S. Semi-automated tracking and continuous monitoring of inferior vena cava diameter in simulated and experimental ultrasound imaging. Ultrasound Med Biol 2015;41:845–57.
[17] Belmont B, Kessler R, Theyyunni N, Fung C, Huang R, Cover M, et al. Continuous inferior vena cava diameter tracking through an iterative Kanade-Lucas-Tomasi-based algorithm. Ultrasound Med Biol 2018;44(12):27932801.
[18] Folino A, Benzo M, Pasquero P, Laguzzi A, Mesin L, Messere A, et al. Vena cava responsiveness to controlled isovolumetric respiratory efforts. J Ultrasound Med 2017;36(10):2113–23.
[19] Mesin L, Pasquero P, Roatta S. Tracking and monitoring pulsatility of a portion of inferior vena cava from ultrasound imaging in long axis. Ultrasound Med Biol 2019;45:1338–43.
[20] Mesin L, Pasquero P, Roatta S. Multi-directional assessment of respiratory and cardiac pulsatility of the inferior vena cava from ultrasound imaging in short axis. Ultrasound Med Biol 2020;46:3475–82.
[21] Policastro P, Mesin L. Estimation of inferior vena cava size from ultrasound imaging in X-plane. Electronics 2024;13(17):3406.
[22] Nakamura K, Tomida M, Ando T, Sen K, Inokuchi R, Kobayashi E, et al. Cardiac variation of inferior vena cava: new concept in the evaluation of intravascular blood volume. Med Ultrason (2001) 2013;40(3):205209.
[23] Sonoo T, Nakamura K, Ando T, Sen K, Maeda A, Kobayashi E, et al. Prospective analysis of cardiac collapsibility of inferior vena cava using ultrasonography. J Crit Care 2015;30(5):945948.
[24] Liu FT, Ting KM, Zhou ZH. Isolation forest. In: Paper presented at: 2008 Eighth IEEE International Conference on Data Mining; 2008. p. Pisa, Italy, p. 413–22.